16C.4 TROPICAL CYCLONE BOUNDARY LAYER SHOCKS AND SHOCK-LIKE STRUCTURES

Christopher J. Slocum * and Wayne H. Schubert
Colorado State University, Fort Collins, Colorado

1. INTRODUCTION

Williams et al. (2013) interpreted the structure of the wind field within the boundary layer of Hurricane Hugo (1989) using an axisymmetric slab boundary layer model. This work shows that the dry dynamics form a "shock-like" structure in the boundary layer inflow that resembles the Hurricane Hugo (1989) observations. In applied mathematics, a shock is the spontaneous development of a discontinuity in a smooth initial condition through the advection of momentum by momentum (LeVeque 2002). For weak solutions of hyperbolic conservation laws, this feature of fluid dynamics is referred to as a Burgers' shock (Whitham 1974).

Previous work on the tropical cyclone boundary layer has not included procedures in the numerics to handle shock development for weak solutions of hyperbolic conservation laws (Rosenthal 1962; Ooyama 1969a,b; Chow 1971; Shapiro 1983; Kepert 2010a,b; Smith 2003; Smith and Montgomery 2008; Smith et al. 2009; Smith and Montgomery 2010; Abarca and Montgomery 2013). This is true in the work of Williams et al. (2013). The authors acknowledge this limitation and introduce the terminology "shock-like." In the slab boundary layer model used to interpret the structure of Hurricane Hugo (1989), the finite-differencing and horizontal diffusion terms prevent the formation of true discontinuities. Since the numerics do not include a shock-capturing or -tracking method (Whitham 1974; Shu 1998; LeVeque 2002; Durran 2010), they discuss the importance of the horizontal diffusion terms in relation to the stability constraint and preventing multivalued solutions from developing.

The purpose of this work is to begin to understand how removing the aforementioned restrictions by solving an overly simplified form of the slab boundary layer model equations through the method of characteristics would impact the results of Williams et al. (2013). We will begin by outlining the slab boundary layer model used by Williams et al. (2013), and then we will present an idealized analytical argument in characteristic form.

2. SLAB BOUNDARY LAYER MODEL

The model considers axisymmetric, boundary layer motions of an incompressible fluid on an f-plane with a constant depth h. The radial and azimuthal velocities are independent of height. The vertical velocity $w(r,t)$ is defined at height h. In the overlying layer the radial velocity is assumed to be negligible and the azimuthal velocity $v_{\rm gr}(r)$ is assumed to be in gradient balance and to be a specified function of radius. The boundary layer flow is driven by the same radial pressure gradient force that occurs in the overlying fluid, so that, in the radial equation of boundary layer motion, the pressure gradient force can be expressed as the specified function $[f + (v_{\rm gr}/r)]v_{\rm gr}$. The governing system of differential equations for the boundary layer variables $u(r,t)$, $v(r,t)$, and $w(r,t)$ then takes the form

$$\begin{aligned}\frac{\partial u}{\partial t} + u\frac{\partial u}{\partial r} + w^-\left(\frac{u}{h}\right) &= \left(f + \frac{v + v_{\rm gr}}{r}\right)(v - v_{\rm gr}) \\ &\quad - c_D U\frac{u}{h} + K\frac{\partial}{\partial r}\left(\frac{\partial(ru)}{r\partial r}\right), \end{aligned} \tag{1}$$

$$\begin{aligned}\frac{\partial v}{\partial t} + u\left(f + \frac{\partial v}{\partial r} + \frac{v}{r}\right) + w^-\left(\frac{v - v_{\rm gr}}{h}\right) \\ = -c_D U\frac{v}{h} + K\frac{\partial}{\partial r}\left(\frac{\partial(rv)}{r\partial r}\right), \end{aligned} \tag{2}$$

$$w = -h\frac{\partial(ru)}{r\partial r} \quad \text{and} \quad w^- = \tfrac{1}{2}(|w| - w), \tag{3}$$

where

$$U = 0.78\left(u^2 + v^2\right)^{1/2} \tag{4}$$

is the wind speed at 10 m height, f the constant Coriolis parameter, and K the constant horizontal diffusivity. The drag coefficient c_D is assumed to depend on the 10 m wind speed according to

$$c_D = 10^{-3}\begin{cases} 2.70/U + 0.142 + 0.0764U & \text{if } U \le 25 \\ 2.16 + 0.5406\left\{1 - \exp[-(U - 25)/7.5]\right\} & \\ & \text{if } U \ge 25, \end{cases} \tag{5}$$

where the 10 m wind speed U is expressed in m s^{-1}. Appendix A of Williams et al. (2013) explains the above derivation of the slab boundary model in greater detail.

The boundary conditions are

$$\left.\begin{aligned} u &= 0 \\ v &= 0 \end{aligned}\right\} \text{ at } r = 0, \qquad \left.\begin{aligned} \frac{\partial(ru)}{\partial r} &= 0 \\ \frac{\partial(rv)}{\partial r} &= 0 \end{aligned}\right\} \text{ at } r = b, \tag{6}$$

where b is the radius of the outer boundary. The initial conditions are

$$u(r,0) = u_0(r) \quad \text{and} \quad v(r,0) = v_0(r), \tag{7}$$

where $u_0(r)$ and $v_0(r)$ are specified functions.

3. IDEALIZED ANALYTICAL ARGUMENT

The formation of shocks in the u and v fields in the hurricane boundary layer depends on the $u(\partial u/\partial r)$ and $u[f + (\partial v/\partial r) + (v/r)]$ terms in (1) and (2), with the term

* *Corresponding author address:* Christopher J. Slocum,
Dept. of Atmos. Sci., Colorado State University, Fort Collins, CO;
e-mail: cslocum@atmos.colostate.edu.

TABLE 1. Test cases and results for idealized analytical argument. [This table is adapted from Slocum (2013) and Slocum et al. (2014).]

Test Case	a (km)	u_m (m s^{-1})	v_m (m s^{-1})	U (m s^{-1})	τ (h)	r_s (km)	t_s (h)
S1	300	-0.5	3.2	2.5	78.6	87.9	No Shock
S2	200	-1.0	6.3	5.0	52.2	58.6	38.7
S3	150	-2.0	12.7	10.0	23.6	44.0	13.4
S4	100	-4.0	25.3	20.0	7.69	29.3	4.52
S5	60	-6.0	38.0	30.0	3.82	17.6	1.69
S6	40	-8.0	50.7	40.0	2.64	11.7	0.791
S7	30	-10.0	63.3	50.0	2.07	8.79	0.457

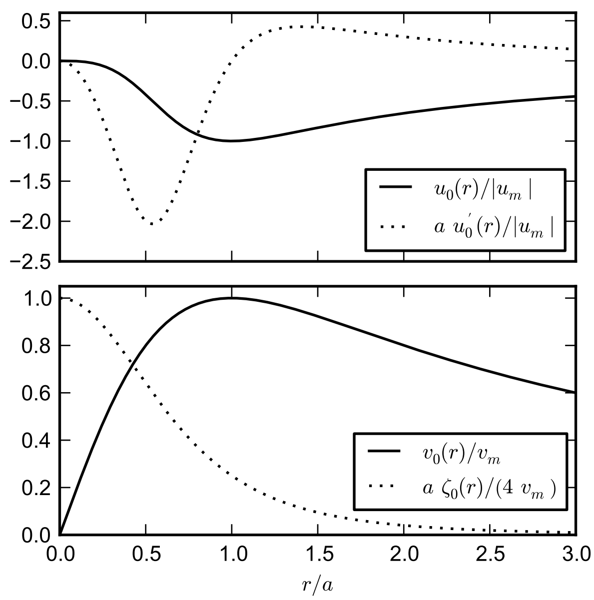

FIG. 1. The dimensionless initial conditions used in the analytical models for the single eyewall cases as computed from equations (17)–(20). The solid line in the upper panel shows the dimensionless initial radial velocity $u_0(r)/|u_m|$ for the case in which $u_m < 0$, while the dotted line shows its dimensionless radial derivative $a\,u_0'(r)/|u_m|$. Similarly, the solid line in the lower panel shows the dimensionless initial tangential velocity $v_0(r)/v_m$, while the dotted line shows the dimensionless initial vorticity $a\,\zeta_0(r)/(4v_m)$. [Figure from Slocum et al. (2014).]

proportional to the agradient tangential flow $(v-v_{\rm gr})$ serving as a forcing mechanism for $(\partial u/\partial t)$, the surface friction terms serving to damp u and v, and the horizontal diffusion terms serving to control the structure near the shock. As we shall see, the shocks in u and v occur at the same time and at the same radius. These discontinuities in the radial and tangential flow mean that there is a circle of infinite vertical velocity at the top of the boundary layer and a circular infinite vorticity sheet in the boundary layer.

To obtain a semi-quantitative understanding of the above concepts using the method of characteristics, we now approximate (1) and (2) by neglecting the horizontal diffusion terms, the w^- terms (Chow 1971; Shapiro 1983), and the $(v-v_{\rm gr})$ forcing term. We keep the surface drag effects and, for simplicity, we linearize the surface drag terms so the radial and tangential momentum equations become

$$\frac{\partial u}{\partial t} + u\frac{\partial u}{\partial r} = -\frac{u}{\tau}, \tag{8}$$

$$\frac{\partial v}{\partial t} + u\left(f + \frac{\partial v}{\partial r} + \frac{v}{r}\right) = -\frac{v}{\tau}, \tag{9}$$

where the constant damping time scale τ is a typical value of $h/(c_D U)$. For the test case S3, the value of τ is 3.82 h which is computed using $h = 1000$ m, $U = 30$ m s^{-1}, and $c_D \approx 2.4\times10^{-3}$ as given by (5). Parameters and results for this and other cases are outlined in Table 1.

While (8) and (9) do not hold up to a rigorous scale analysis of the tropical boundary layer, as previously noted, in the absence of the horizontal diffusion terms, the slab boundary layer equations constitute a hyperbolic system. To solve the hyperbolic system, we must know the boundary conditions (7) as well as the initial condition. If the $(v-v_{\rm gr})$ forcing term is not neglected, we also need to know how the forcing influences the information along a characteristic in time. The simplifications made to (1) and (2) allow us to explore how one set of characteristics influences the structure of the tropical cyclone boundary layer.

The solutions of (8) and (9) are easily obtained by noting that these two equations can be written in the form

$$\frac{d}{dt}\left\{ue^{t/\tau}\right\} = 0, \tag{10}$$

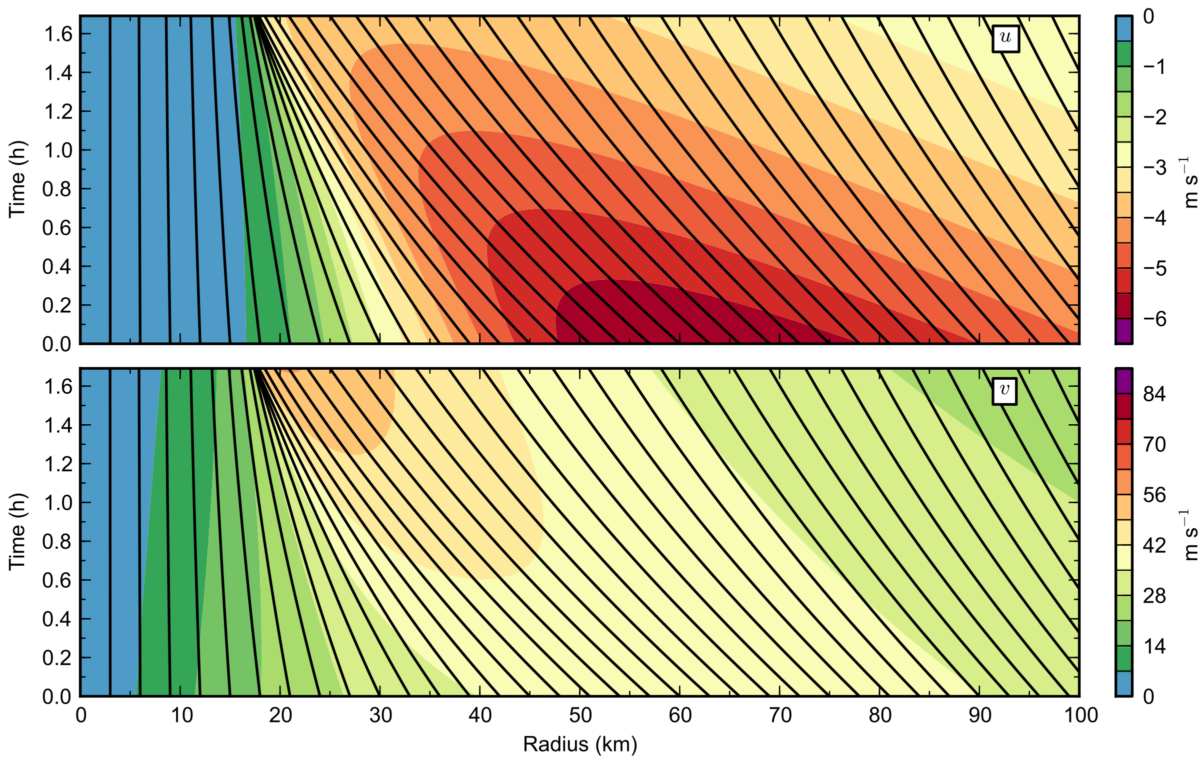

FIG. 2. The analytical solutions $u(r,t)$ and $v(r,t)$ (color contours), as well as the characteristic curves (black curves on each panel). These solutions are for the particular initial conditions (17) and (18) for the case when $a = 60$ km, $u_m = -6$ m s^{-1}, $v_m = 38$ m s^{-1}. The plots cover the time interval $0 \le t \le t_s$, where $t_s = 1.69$ h is the shock formation time for this particular initial condition. [Figure from Slocum et al. (2014).]

$$\frac{d}{dt}\left\{rve^{t/\tau} + f\left[\hat{r}t + u_0(\hat{r})\tau(t-\hat{t})\right]u_0(\hat{r})\right\} = 0, \quad (11)$$

where $(d/dt) = (\partial/\partial t) + u(\partial/\partial r)$ is again defined as the derivative following the boundary layer radial motion, and where the characteristics $\hat{r}(r,t)$ are given implicitly by

$$r = \hat{r} + \hat{t}u_0(\hat{r}), \quad (12)$$

with the function $\hat{t}(t)$ defined by

$$\hat{t} = \tau\left(1 - e^{-t/\tau}\right). \quad (13)$$

The derivatives of $(\partial u/\partial t)$ and $(\partial u/\partial r)$ become infinite when

$$tu_0'(\hat{r}) = -1 \quad (14)$$

along one or more characteristics. We can use this information to determine when and where a shock will form through combining (13) and (14) to solve for the time of shock formation, which is

$$t_s = -\tau\ln\left(1 + \frac{1}{\tau u_0'(\hat{r}_s)}\right), \quad (15)$$

and the radius of shock formation, determined from (12) and (14), which is

$$r_s = \hat{r}_s - \frac{u_0(\hat{r}_s)}{u_0'(\hat{r}_s)}. \quad (16)$$

As a simple example, consider the initial conditions

$$u_0(r) = u_m\left(\frac{4(r/a)^3}{1+3(r/a)^4}\right), \quad (17)$$

$$v_0(r) = v_m\left(\frac{2(r/a)}{1+(r/a)^2}\right), \quad (18)$$

where the constants a, u_m, and v_m specify the radial extent and strength of the initial radial and tangential flow. The derivative of (17) is

$$u_0'(r) = \frac{12u_m}{a}\left(\frac{(r/a)^2[1-(r/a)^4]}{[1+3(r/a)^4]^2}\right), \quad (19)$$

while the initial relative vorticity, obtained by differentiation of (18), is

$$\zeta_0(r) = \frac{4v_m}{a\left[1+(r/a)^2\right]^2}. \quad (20)$$

The dimensionless forms of (17)–(20) are shown in Fig. 1.

For the initial conditions (17)–(20), the solutions take the form

$$u(r,t) = u_m\left(\frac{4(\hat{r}/a)^3 e^{-t/\tau}}{1+3(\hat{r}/a)^4}\right), \quad (21)$$

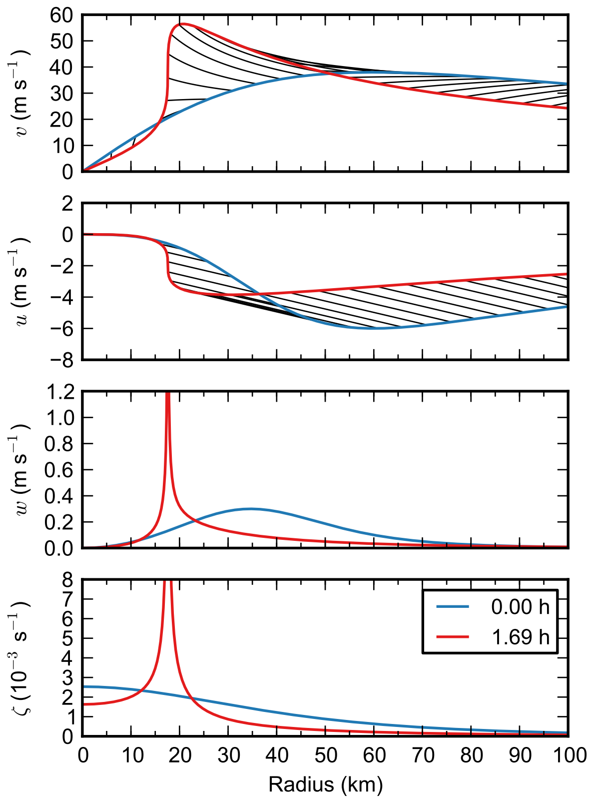

FIG. 3. The radial profiles of v, u, w, ζ at $t = 0$ (blue) and at $t = t_s = 1.69$ h (red). Also shown by the black curves in the top two panels are fluid particle displacements for particles that are equally spaced at the initial time. At $t = t_s$, the u and v fields become discontinuous at $r = r_s = 17.6$ km, while the w and ζ fields become singular there. [Figure from Slocum et al. (2014).]

$$rv(r,t) = \left\{ \hat{r} v_m \left(\frac{2(\hat{r}/a)}{1 + (\hat{r}/a)^2} \right) + f \frac{t}{\hat{t}} \left[\hat{r} + (r - \hat{r}) \left(\frac{\tau(t - \hat{t})}{t\hat{t}} \right) \right] (\hat{r} - r) \right\} e^{-t/\tau}, \quad (22)$$

where the characteristic curves (along which $\hat{r}$ is fixed) are defined by

$$r = \hat{r} + u_m \hat{t} \left(\frac{4(\hat{r}/a)^3}{1 + 3(\hat{r}/a)^4} \right). \quad (23)$$

The solutions for $u(r,t)$, $v(r,t)$, $\hat{r}(r,t)$, as given by (21)–(23), are plotted in the two panels of Fig. 2 for the case when $a = 60$ km, $u_m = -6$ m s^{-1}, $v_m = 38$ m s^{-1}. The plots cover the radial interval $0 \le r \le 100$ km and the time interval $0 \le t \le t_s$, where $t_s = 1.69$ h is the shock formation time for this particular initial condition. Another view of this analytical solution is given in Fig. 3, with the four panels displaying the radial profiles (at $t = 0$ in blue and at $t = t_s$ in red) of u, v, w, ζ. Also shown by the black curves in the top two panels are fluid particle displacements for particles that are equally spaced at the initial time. At $t = t_s$, the u and v fields become discontinuous at $r = 17.6$ km, while the w and ζ fields become singular there.

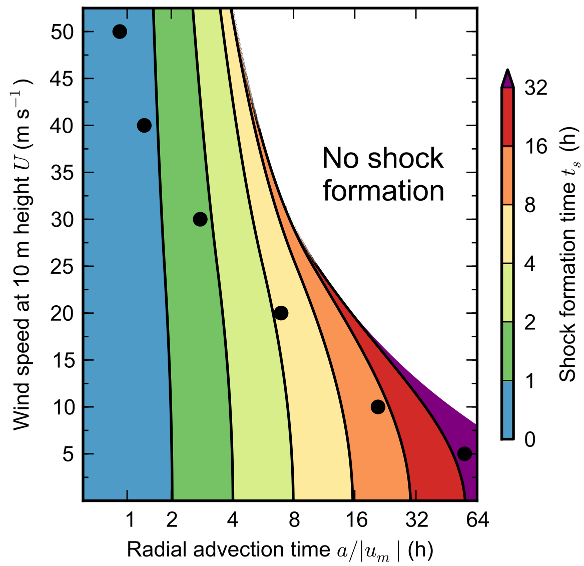

FIG. 4. Isolines of the shock formation time t_s (with color scale at right) computed from (15) as a function of the radial advection time $a/|u_m|$ and the 10 m wind speed U. The six dots correspond to the strength U and size a of typical tropical cyclones. The white region shows where shocks do not form. [Figure from Slocum et al. (2014).]

For the hurricane strength vortices, the shock formation time is generally less than 1 hour. Since $\tau = h/(c_D U)$, (15) can also be regarded as giving the shock formation time t_s as a function of the radial advection time $a/|u_m|$ and the 10 m wind speed U. Contours of t_s are shown in Fig. 4. The ordinate is the boundary layer wind speed that can be used to determine the strength of the tropical cyclone, U. The abscissa is the radial advection time, which is defined by the radius of maximum wind, a, divided by the maximum radial velocity, $|u_m|$. More intense storms are located near the upper left corner of the figure; weak tropical storms are in the lower right corner of the plot. The six dots correspond to typical values of a and U for various strength vorticies as noted in Table 1.

4. DISCUSSION AND CONCLUDING REMARKS

While the idealized analytical arguments presented here neglect the horizontal diffusion terms, the w^- terms, and the $(v - v_{\rm gr})$ terms, (8) and (9) do provide valuable insight into how to interpret the dynamics involved in boundary layer shocks. Figs. 2 and 3 show that information originating from a smooth initial condition will develop discontinuities in u and v. The corresponding singularities in w and ζ provide insight into what determines the size of an eye and how potential vorticity rings are produced through nonlinear processes. While the singularities may seem unrealistic, moist dynamics associated with the eyewall would act to lessen w and ζ to values seen in Williams et al. (2013). The idealized analytical argument also is limited by the fact that the shock originates solely from the smooth initial condition for the radial velocity defined by (17) in the absence of the $(v - v_{\rm gr})$ forcing term. Returning to (1) and (2), the agradient tangential flow will act as a forcing mechanism for $(\partial u/\partial t)$. However, it is encouraging to see similar structures develop in the Williams et al. (2013) solutions.

Fig. 4 shows that hurricane strength vorticies will quickly generate and maintain a shock. The figure suggests that shocks will develop over long periods of time in tropical storms, but as storms intensify, the shocks develop rapidly. However, the threshold for shock development is small based on the radial advection time associated with strong tropical cyclones. This potentially offers insight into how a process like landfall can cause a vortex to weaken. If landfall increases the radial advection time of a storm, a shock may not redevelop and the mechanism, producing the potential vorticity ring and maintaining the eye, would dissipate.

In comparing the idealized analytical argument to previous work, the characteristic form of (1)–(7) without the diffusion terms is a weak solution of a hyperbolic system. As such, the system cannot be solved as a steady-state problem. Even though Williams et al. (2013) includes diffusion, the numerical solutions should be considered as reaching quasi-steady-state. As shown by Fig. 2, characteristics containing information from the initial condition and the boundary conditions are still contributing and changing the solution. When the $(v - v_{\rm gr})$ forcing term is included, the characteristics accrue information associated with the forcing. The fact that a hyperbolic system requires knowledge from all four information sources means the system cannot be regarded as steady-state. Trying to integrate inward from the outer boundary condition at $r = b$ to find the steady-state solution will result in u and v becoming singular or in spurious oscillations as seen in Smith (2003) and Kepert (2010a,b). In order to solve the hyperbolic time dependent system of equations numerically, a shock-capturing or -tracking procedure must be included to compute solutions past t_s. These procedures and methods are briefly outlined in (Whitham 1974; Shu 1998; LeVeque 2002; Durran 2010).

Acknowledgments

We would like to thank Mark DeMaria, Rick Taft, Alex Gonzalez, Gabriel Williams, Paul Ciesielski, Hugh Willoughby, Michael Fiorino, Joseph Biello, and Greg Holland for their comments. This research has been supported by the Hurricane Forecast Improvement Project (HFIP) through the Department of Commerce (DOC) National Oceanic and Atmospheric Administration (NOAA) Grant NA090AR4320074 and through the National Science Foundation under Grants ATM-0837932 and AGS-1250966 and under the Science and Technology Center for Multi-Scale Modeling of Atmospheric Processes, managed by Colorado State University through cooperative agreement No. ATM-0425247. The calculations were made on high-end Linux workstations generously provided through a gift from the Hewlett-Packard Corporation.

REFERENCES

Abarca, S. F. and M. T. Montgomery, 2013: Essential dynamics of secondary eyewall formation. *J. Atmos. Sci.*, **70**, submitted.

Chow, S., 1971: A study of the wind field in the planetary boundary layer of a moving tropical cyclone. M.S. thesis, Dept. of Meteor. and Oceanogr. New York University, 59 pp.

Durran, D. R., 2010: *Numerical Methods for Fluid Dynamics*. 2d ed., Springer, 516 pp.

Kepert, J. D., 2010a: Slab- and height-resolving models of the tropical cyclone boundary layer. Part I: Comparing the simulations. *Quart. J. Roy. Meteor. Soc.*, **136**, 1686–1699.

Kepert, J. D., 2010b: Slab- and height-resolving models of the tropical cyclone boundary layer. Part II: Why the simulations differ. *Quart. J. Roy. Meteor. Soc.*, **136**, 1700–1711.

LeVeque, R. J., 2002: *Finite volume methods for hyperbolic problems*. Cambridge University Press, 558 pp.

Ooyama, K., 1969a: Numerical simulation of the life cycle of tropical cyclones. *J. Atmos. Sci.*, **26**, 3–40.

Ooyama, K., 1969b: Numerical simulation of tropical cyclones with an axi-symmetric model. *Proc. Third Symposium on Numerical Weather Prediction*, Tokyo, WMO/IUGG, 81–88.

Rosenthal, S. L., 1962: A theoretical analysis of the field of motion in the hurricane boundary layer. National Hurricane Project Report No. 56, 12 pp.

Shapiro, L. J., 1983: The asymmetric boundary layer flow under a translating hurricane. *J. Atmos. Sci.*, **40**, 1984–1988.

Shu, C.-W., 1998: Essentially non-oscillatory and weighted essentially non-oscillatory schemes for hyperbolic conservation laws. *Advanced numerical approximation of non-linear hyperbolic equations*, B. Cockburn, C. Johnson, C.-W. Shu, and E. Tadmor, Eds., Springer, No. 1697 in Lecture notes in mathematics, a. quarteroni ed., 325–432.

Slocum, C. J., 2013: Diabatic and frictional forcing effects on the structure and intensity of tropical cyclones. M.S. thesis, Dept. of Atmos. Sci., Colorado State University, 77 pp., [Available from Colorado State University, 1019 Campus Delivery, Fort Collins, CO 80523-1019.].

Slocum, C. J., G. J. Williams, R. K. Taft, and W. H. Schubert, 2014: Tropical cyclone boundary layer shocks. *J. Adv. Model. Earth Syst.*, **6**, submitted.

Smith, R. K., 2003: A simple model of the hurricane boundary layer. *Quart. J. Roy. Meteor. Soc.*, **129**, 1007–1027.

Smith, R. K. and M. T. Montgomery, 2008: Balanced boundary layers in hurricane models. *Quart. J. Roy. Meteor. Soc.*, **134**, 1385–1395.

Smith, R. K. and M. T. Montgomery, 2010: Hurricane boundary-layer theory. *Quart. J. Roy. Meteor. Soc.*, **136**, 1665–1670.

Smith, R. K., M. T. Montgomery, and S. V. Nguyen, 2009: Tropical cyclone spin-up revisited. *Quart. J. Roy. Meteor. Soc.*, **135**, 1321–1335.

Whitham, G. B., 1974: *Linear and Nonlinear Waves*. John Wiley and Sons, 363 pp.

Williams, G. J., R. K. Taft, B. D. McNoldy, and W. H. Schubert, 2013: Shock-like structures in the tropical cyclone boundary layer. *J. Adv. Model. Earth Syst.*, **5**, 338–353, doi:10.1002/jame.20028,2013.